

## Percolation in an interactive cluster-growth model

Scott R. Anderson and Fereydoon Family

*Department of Physics, Emory University, Atlanta, Georgia 30322*

(Received 17 March 1988)

Interactions are included in the standard model of site percolation by specifying two numbers,  $p_0$  and  $p_1$ , which are the probabilities of occupying a site on a lattice if none or at least one of the neighboring sites are occupied, respectively. This is expected to be a better description of systems where interactions between neighbors can either enhance or deter site occupation. Monte Carlo methods are used to simulate the irreversible growth of clusters starting from an empty two-dimensional square lattice, and continuing through the percolation threshold. The value of the percolation threshold  $p_c$  and other properties of the system depend on the parameter  $r = p_1/p_0$ . For  $r = 1$ , the system corresponds to random percolation. As  $r \rightarrow \infty$ , compact Eden clusters are produced, which link together to form larger, fractal clusters. As  $r \rightarrow 0$ , neighboring sites become less easily occupied, resulting in checked "domains" separated by antiphase boundaries. Several quantities are analyzed to determine the critical exponents  $\nu$ ,  $\gamma$ , and  $\beta$ , including the threshold distribution width, the mean cluster size, and the infinite cluster size. For all finite values of  $r$ , the data are found to be consistent with the exponents of random percolation.

### I. INTRODUCTION

The formation of many disordered systems can be described by a growth process in which individual elements randomly join together to form an interconnected, percolating network. Important examples include the gelation of polymeric materials<sup>1,2</sup> and the growth of islands on surfaces via atomic chemisorption.<sup>3</sup> The most widely used model for such systems is the percolation model,<sup>4</sup> in which sites (or bonds) on a lattice are occupied with a probability  $p$ , independent of the occupation of the neighboring sites. Nearest-neighbor sites are then considered to be connected, resulting in clusters of varying sizes and geometries. If the probability  $p$  is large enough,  $p > p_c$ , one cluster will percolate through the entire lattice. This "infinite" cluster corresponds to a gel in gelation, or to a conduction path through metallic atoms across a surface. Its formation signals a geometric phase transition, and the region around  $p_c$  can be analyzed for scaling behavior and critical exponents.

In general, however, a physical system will have some type of interaction between its individual elements. In surface deposition, for example, the presence of neighbors can either enhance or deter absorption at a site. Such interactions will give rise to correlations which can affect the properties of the system in important ways. Several methods have therefore been proposed to introduce interactions into the percolation model,<sup>1</sup> the most studied of which utilizes Ising correlation.<sup>5</sup>

In this paper, a different type of interactive percolation is considered.<sup>6</sup> The basic model, along with several variations, was previously discussed by Evans, Bartz, and Sanders<sup>7</sup> in the context of cluster growth and statistics before coalescence. It differs from Ising-correlated percolation in that the interactions are introduced in a way that is a simple generalization of random site percolation. Instead of using a single probability  $p$  to decide if a site

should be occupied, two probabilities are used,  $p_0$  and  $p_1$ , according to whether the site has no neighbors or at least one neighbor, respectively. The concentration  $p$  is then a function of  $p_0$  and  $p_1$ , and random percolation is recovered when  $p_0 = p_1$ . Because the occupation of a site now depends on the state of its neighbors, the site must be chosen randomly. If the lattice is initially empty, clusters will then be nucleating with a probability  $p_0$ , and growing site-by-site at their perimeters with a probability  $p_1$ . This picture invites direct comparison with atomic chemisorption on surfaces, where the deposited particles randomly form islands which then grow and coalesce.<sup>3</sup> The analogy can be extended by requiring irreversible growth, and by allowing sites to be visited more than once. The concentration  $p$  will then monotonically increase from zero, pass through a percolation threshold  $p_c$ , and eventually saturate. The threshold  $p_c$ , the mean cluster size  $S$ , and other properties of the system will depend on  $p_0$  and  $p_1$ , and will in general differ from their random percolation values.

Of particular interest is the effect of the interactions on the critical phenomena at  $p_c$ , i.e., whether or not they will change the universality class. As is well known, the behavior of a system at a critical point is due to the presence of a diverging length scale, before which all other lengths become unimportant. For percolation, this length scale is the connectivity length  $\xi$ , i.e., the range over which two sites are likely to be part of the same cluster. Modification of the critical exponents would then be expected to occur only if the correlation length of the interactions  $\tilde{\xi}$  is also divergent, so that a competition can occur between  $\xi$  and  $\tilde{\xi}$ . In Ising-correlated percolation, for example, it has been found that in two dimensions, where the thermal critical point  $T = T_c$ ,  $p = 0.5$  coincides with the percolation threshold  $p_c(T_c)$ , the exponents do, indeed, differ from those of random percolation.<sup>5</sup> It is quite possible, then, that a similar situation

might exist in the correlated cluster-growth model presented here, although it may again be limited to a single point in the phase diagram.

In the next section, the general characteristics of the cluster-growth model of interactive percolation are described, and its universality class is discussed. Arguments are presented which limit any differences from random percolation to the single point  $r = \infty$ . In Sec. III, numerical calculations of many of the properties of the model at the percolation threshold are presented, and the critical exponents are estimated for a range of finite  $r$ . As argued, the exponents are found to be consistent with those of random percolation. The conclusions are set forth in Sec. IV.

## II. CHARACTERIZATION OF THE MODEL

In general, the properties of the model, such as the concentration  $p$ , will depend on the parameters  $p_0$  and  $P_1$ , and on the time  $t$ . Because  $p$  is a monotonic function of time, however, it may be used in place of  $t$ . To characterize the state of the system, it is then only necessary to specify, in addition, the ratio  $r = p_1/r_0$ , since a uniform scaling of  $p_0$  and  $p_1$  will affect only the time it takes to arrive at the concentration  $p$ . The phase diagram then appears as in Fig. 1, which shows the dependence of the percolation threshold  $p_c$  on  $r$ .

When  $r > 1$ , the site occupation will be "ferromagnetic" in nature, since sites that have occupied neighbors will be preferred over those that do not. Cluster nucleation will therefore be small, resulting in widely separated clusters which can then grow radially in an Eden-like manner.<sup>8</sup> Eventually, these compact Eden clusters, or "blobs,"<sup>2</sup> will link together and form large, fractal clusters,<sup>9</sup> one of which will percolate through the system. This can be observed in Fig. 2, which shows the distribution of clusters at the percolation threshold for several values of  $r$ . In each case, the infinite cluster is shown in black, with all other clusters in gray; the blobs are easily distinguishable for  $r \gtrsim 100$ . The average blob size is seen to be an increasing function of  $r$ , while the density of blobs is a decreasing function. The overall concentration of occupied sites also appears to be smaller, in accordance with the decrease in  $p_c$  observed in Fig. 1. A similar decrease in  $p_c$  as the interaction strength increases is observed in ferromagnetic Ising-correlated systems.<sup>10</sup>

When  $r < 1$ , on the other hand, the site occupation will be "antiferromagnetic" in nature, since the presence of occupied neighbors will be inhibitory. Initially, therefore, there will be many single-particle blobs, which will only link together with difficulty. They will tend to lie on one of two sublattices, forming next-nearest-neighbor-connected domains separated by antiphase boundaries. This is more easily seen when comparing with random percolation in Fig. 2. The concentration is also noticeably greater as is reflected in Fig. 1. Again, this is similar to the increase in  $p_c$  observed in antiferromagnetic Ising-correlated systems as the interaction strength increases.<sup>11</sup>

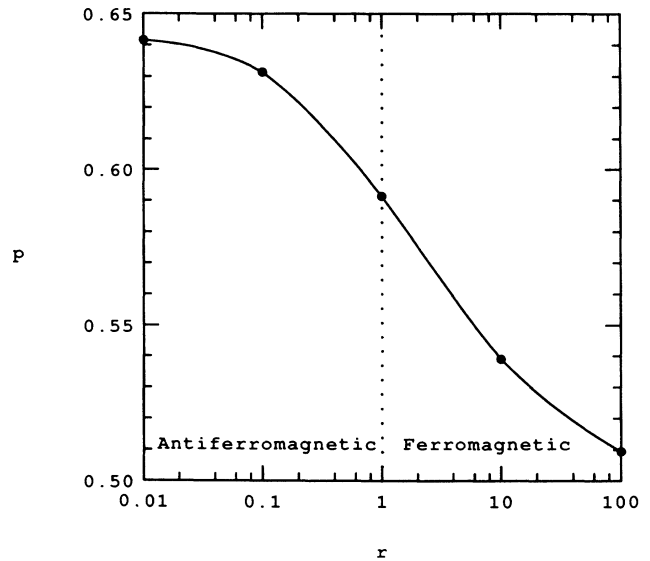


FIG. 1. The phase diagram of the cluster-growth model of interactive percolation, showing the percolation threshold concentration as a function of  $r = p_1/p_0$ . Below  $r = 1$ , the random percolation value, the system behaves antiferromagnetically; above, it is ferromagnetic.

At first glance, the percolative structures shown in Fig. 2 appear to be very different from each other. Consider, however, when the value of  $r$  is large, and, instead of the original particles, the blobs are taken to be the basic elements which join together to form percolating clusters. Then, these pictures are very similar to random percolation (on a smaller lattice). This suggests that as long as all quantities are scaled by the linear blob size  $R_0$ , the properties of the system will not change. Then the critical behavior will be independent of  $r$ , and the universality class will remain that of random percolation. Nonuniversal quantities may differ, however, such as the percolation threshold  $p_c$  in Fig. 1 (the decrease of  $p_c$  as  $r$  increases is, in fact, expected, because the blobs have an increasing coordination number<sup>4,12</sup>  $z \sim R_0^{(d-1)}$ ). This renormalization argument should also hold for smaller  $r$ , even though the blobs are not so easily distinguishable. The only place where it might break down is for  $r = \infty$ , since there  $R_0 = \infty$  also.

What, then, is the effect of the interactions? As discussed previously, they control the growth of the blobs, once they have nucleated. However, they are not really involved in linking the blobs together; this is strictly a connectivity property resulting from the random placement of the nucleating sites, which are ultimately of a certain size. The correlation length, therefore, should be comparable to the blob size  $\xi \sim R_0$ , and will only diverge when  $r = \infty$ . The universality class will not then be changed for all  $r < \infty$ , in agreement with the preceding discussion. This picture of the blobs as noninteracting percolating elements makes the model here, for very large  $r$ , similar to the continuum percolation problem with a distribution of disk sizes.<sup>13</sup> In that problem, the critical

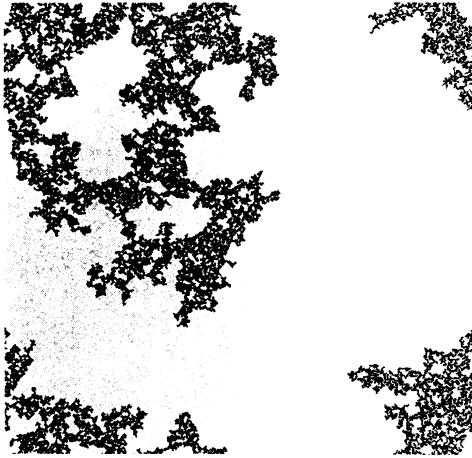
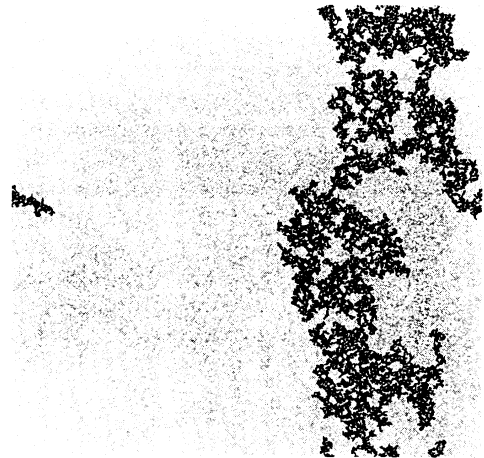
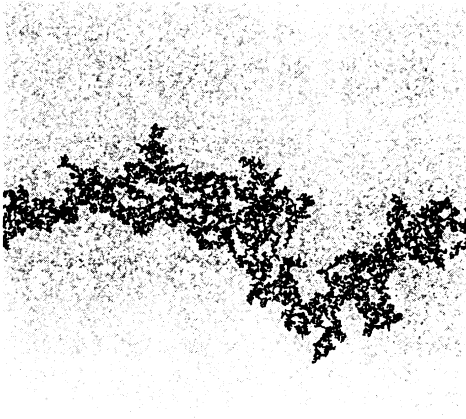
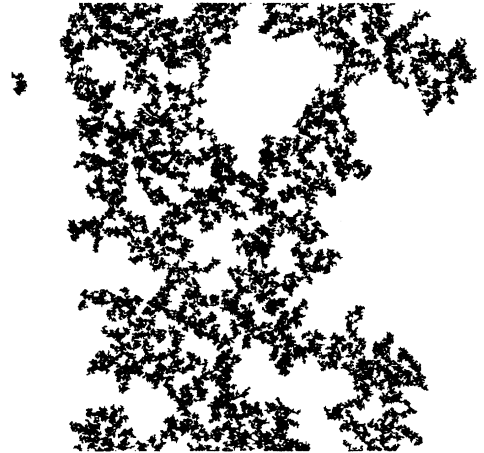
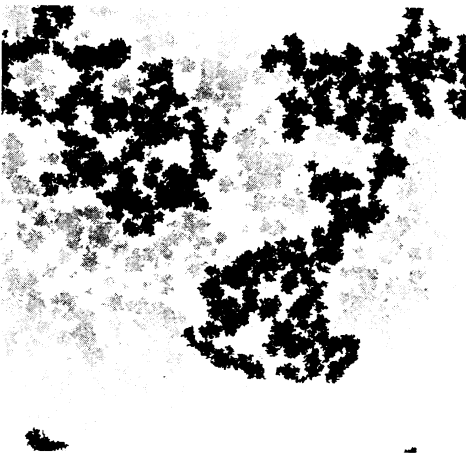
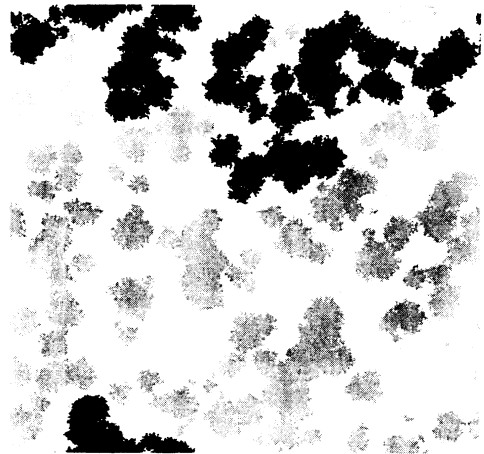
(a)  $r = 0.001$ (b)  $r = 1$ (c)  $r = 10$ (d)  $r = 100$ (e)  $r = 1000$ (f)  $r = 10\,000$ 

FIG. 2. Sample cluster distributions at the percolation threshold. The infinite cluster is black; all others are gray. (a)  $r = 0.001$ ; (b)  $r = 1$ ; (c)  $r = 10$ ; (d)  $r = 100$ ; (e)  $r = 1000$ ; (f)  $r = 10\,000$ .

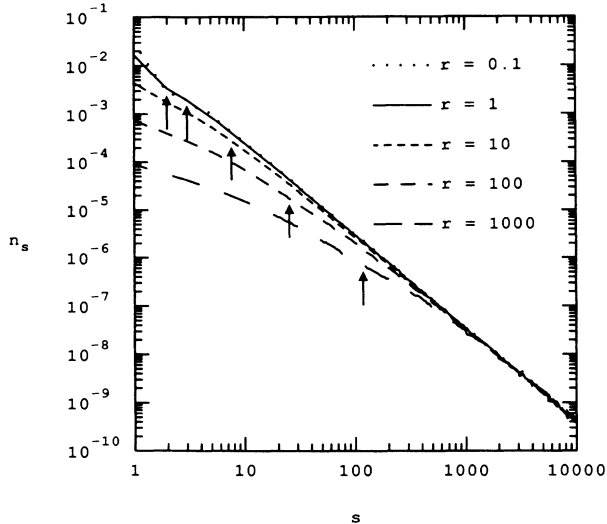


FIG. 3. The cluster-size distribution  $n_s$ , for several values of  $r$ . The data are for a lattice of size  $L = 512$ . The arrows show the associated blob size  $s_0$  for each  $r$ .

exponents were also found to be unchanged from those of ordinary random percolation.

These considerations can be illustrated more quantitatively by examining the cluster size distribution  $n_s$  which is shown at the percolation threshold in Fig. 3. For each curve  $r \geq 1$ , the arrows point to the appropriate blob size  $s_0$  (as calculated in Sec. III). Two effects are apparent from this figure. The first is that, as  $s/s_0 \rightarrow \infty$ ,  $n_s$  becomes independent of  $s_0$ . In other words, the number of very large clusters  $s \gg s_0$  does not depend on the size of the blobs which make them up. This shows the relative unimportance of the blob size at larger length scales, and in particular at the critical point where the connectivity length  $\xi$  is diverging. The other effect is the variation in the curves when  $s \lesssim s_0$ . For  $r < 1$ , the only difference from random percolation is a slight increase in the number of clusters present at small  $s$ . This is related to the larger concentration at  $p_c$  in the antiferromagnetic regime (see Fig. 1), since  $p = \sum_s s n_s$  for  $p \leq p_c$ . For  $r > 1$ , the number of clusters present for small  $s$  is greatly reduced, which is to be expected since most of the clusters are either the blob size  $s_0$  or larger (composite). This is responsible for the reduction in critical concentration when  $r$  is large.

The above argument are intended to establish the plausibility of the random percolation universality class for this model. In Sec. III, Monte Carlo simulations and a finite-size scaling analysis are used to support this conclusion.

### III. NUMERICAL RESULTS

The simulations of this cluster-growth model were carried out using standard Monte Carlo techniques<sup>14</sup> on a square lattice with periodic boundary conditions, using sizes  $L = 16-512$  and values of  $r = 0.01-1000$ . The num-

ber of runs (i.e., configurations) that were averaged over varied from 32 000 for  $L = 16$  to 2000 for  $L = 512$ . The percolation threshold was determined using two spanning rules, the first using either bottom-to-top or left-to-right spanning of the lattice by a cluster to define  $p_{c1}$ , and the second requiring spanning to occur in both directions, defining  $p_{c2}$ .<sup>15</sup> The quantities discussed below which are functions of  $p(t)$  were all calculated at a particular time and then averaged. The various critical quantities, however, were calculated at criticality and averaged (the time of criticality varies from run to run).

The major focus of this section is the calculation of the critical exponents of the model. For this purpose, the same scaling relations are used as are usually defined for random percolation.<sup>4</sup> However, the discussion of renormalization in Sec. II indicates that instead of the single particles used in random percolation, the percolation here is based on the compact blobs which are qualitatively visible in Fig. 2 for large  $r$ . These blobs have some bulk size  $s_0$ , and a linear size  $R_0$  defined by

$$R_0 = s_0^{1/d}, \quad (3.1)$$

since the blobs are compact Eden clusters. Therefore, whenever a bulk size  $s$  or a linear size  $R$  appears in the random percolation scaling relations, it is expected that the same relations should apply to the present model with  $s$  replaced by  $s/s_0$  and  $R$  replaced by  $R/R_0$ . The numerical results will then provide an important test of this renormalization assumption.

The average blob size  $s_0$  can be quantitatively defined through the relation

$$p = s_0 n_0, \quad (3.2)$$

where  $n_0$  is the number of blobs per unit volume, i.e., the concentration of nucleating sites. Figure 4 shows  $R_0$  as a function of  $r$  at  $p_c$  (extrapolated to  $L = \infty$ ). When  $r = 1$ , it is seen that the blob size is not one, as might first be ex-

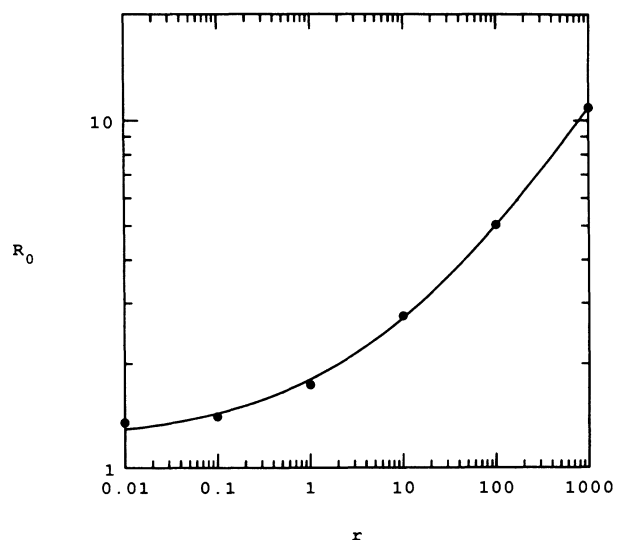


FIG. 4. The linear blob size  $R_0$  as a function of  $r$ .

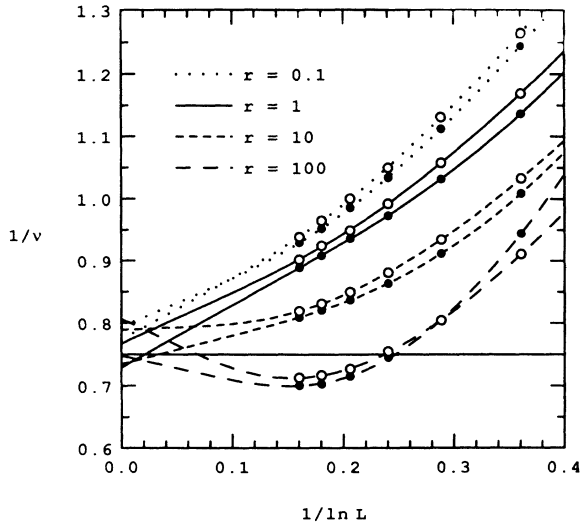


FIG. 5. Finite-size-scaling analysis for the connectivity exponent  $1/\nu$ . Solid circles are the values at  $p_{c1}$ ; open circles are measured at  $p_{c2}$ . The horizontal line indicates the accepted value,  $1/\nu = \frac{3}{4}$ .

pected; this is because a blob can form through random occupation of neighboring sites as well as through enhanced occupation.  $R_0 = 1$  is therefore only expected for  $r \equiv 0$  ( $p_1 = 0$ ). For  $r \gg 1$ , it appears that  $R_0$  increases algebraically with  $r$ ,  $R_0 \sim r^\omega$ . Such a result, with  $\omega = \frac{1}{3}$ , was predicted by Evans, Bartz, and Sanders<sup>7</sup> in their analysis of the cluster statistics of this model. A non-

linear fit to  $R_0$  (shown in Fig. 4) yields an exponent  $\omega = 0.40 \pm 0.04$ , which is close to this value; better data at larger  $r$  may improve the agreement. It should be noted that the blob size for  $r = 1000$ ,  $R_0 \approx 11$ , is large enough to unduly affect the data collected for lattice sizes up to  $L = 128$  [see Fig. 2(e)]. The remaining two sizes examined,  $L = 256$  and  $512$ , will not, therefore, provide results of much precision.

Because of the finite size of the lattices used, the percolation threshold has a distribution of values about its average value, given by a width  $W(L) = [\langle p_c(L)^2 \rangle - \langle p_c(L) \rangle^2]^{1/2}$ . Finite-size scaling arguments<sup>4,16</sup> equate the connectivity length  $\xi \sim (p_c - p)^{-\nu}$  with the lattice size  $L$ , resulting in the relations

$$W(L) \sim p_c(\infty) - p_c(L) \sim L^{-1/\nu}. \quad (3.3)$$

The data for the distribution width  $W$  therefore provide a direct determination of the critical exponent  $\nu$ . The standard analysis<sup>12,15</sup> defines an  $L$ -dependent exponent  $\nu_L$ , which approaches the correct value  $\nu$  as  $L \rightarrow \infty$

$$\frac{1}{\nu_L} \equiv \frac{-\ln W}{\ln L} = \frac{1}{\nu} + \frac{1}{\ln L} [\text{const} + O(L^{-\mu})]. \quad (3.4)$$

When  $1/\nu_L$  is plotted versus  $1/\ln L$ , the data should then lie asymptotically close to a straight line, with a small amount of curvature due to the correction-to-scaling term  $O(L^{-\mu})$ . The results of this analysis are shown in Fig. 5, for both definitions of the percolation threshold  $p_c$ . Although there is some amount of scatter, the data are all consistent with the random percolation value<sup>4</sup>

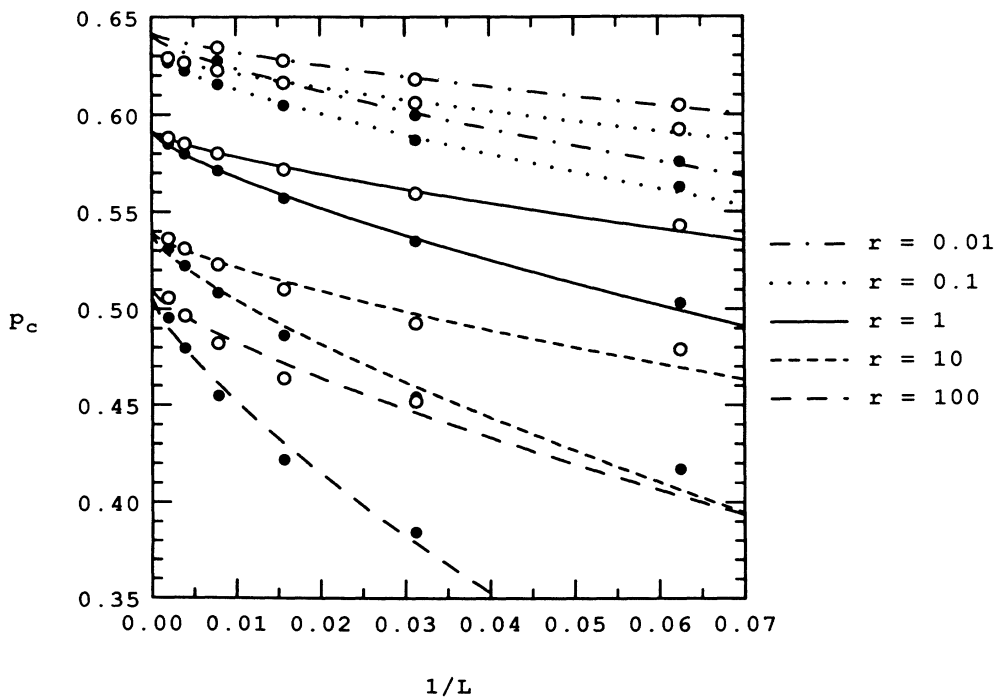


FIG. 6. Finite-size-scaling analysis for the percolation threshold  $p_c$ . Solid circles are the values at  $p_{c1}$ ; open circles are measured at  $p_{c2}$ .

$1/\nu = \frac{3}{4}$ , which is indicated by the horizontal line. It is interesting to note that the result for  $r=100$ ,  $1/\nu = 0.78 \pm 0.03$ , is very close to  $\frac{3}{4}$  despite the significant curvature present. The latter is presumably due to the finite-size effects that become more important as the blob size increases.

For simplicity, it will now be assumed that the value  $\nu = \frac{4}{3}$  is appropriate for all values of  $r$ . It can then be put back into (3.3) to determine  $p_c(\infty)$ . The extrapolations to  $L = \infty$  are shown in Fig. 6 for each value of  $r$  [the resulting values  $p_c(\infty, r)$  were shown in Fig. 1]. It is clear from these figures that the percolation threshold has a strong dependence on  $r$ ; small variations in the value  $\nu$  used, such as those seen in Fig. 5, do not change this conclusion.

The next quantity to be examined is the average cluster size  $S$ , defined by

$$S = \frac{\sum_s s^2 n_s}{\sum_s s n_s} \quad (3.5)$$

Near  $p_c$ ,  $S$  is expected to diverge as<sup>4</sup>

$$S \sim s_0 |p_c - p|^{-\gamma} \quad (3.6)$$

The dependence on  $s_0$  is clearly seen in Fig. 7, which shows  $S$  as a function of  $p$  for several different values of  $r$ . In addition to the increase in peak height as  $r$ , and hence  $s_0$ , increases, it can also be seen that the peak position decreases with  $r$ , which is further verification of the results of Figs. 1 and 6. In a finite system,

$$S(p_c) \sim s_0 \left[ \frac{L}{R_0} \right]^{\gamma/\nu} \sim R_0^d - \gamma/\nu L^{\gamma/\nu} \quad (3.7)$$

so that that the critical exponent ratio  $\gamma/\nu$  can be determined from the  $L$  dependence in the same way as  $\nu$ . For

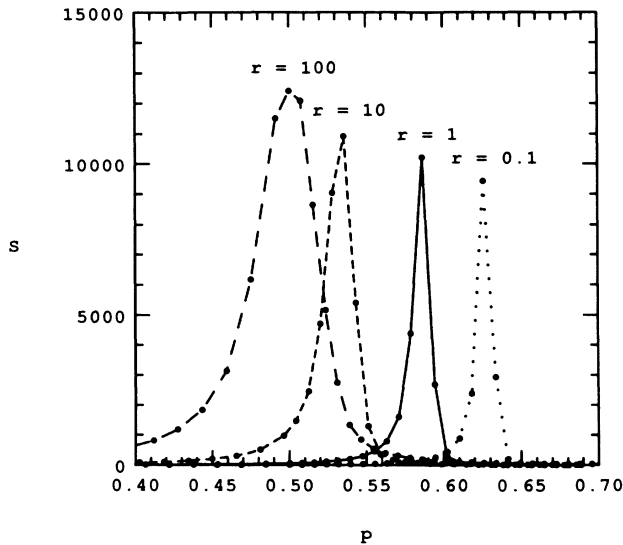


FIG. 7. The average cluster size  $S$  as a function of  $p$ , for several values of  $r$ . The results shown are for a lattice of size  $L = 512$ .

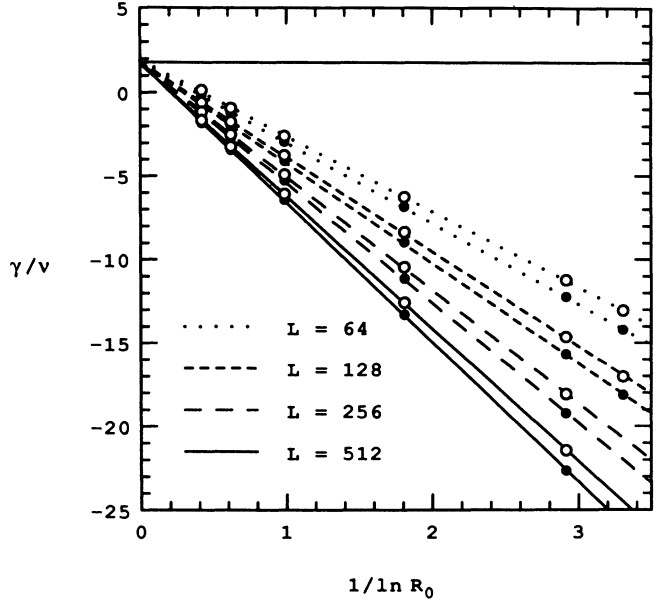


FIG. 8. Finite-size scaling analysis for the cluster-size exponent  $\gamma/\nu$ . Filled circles are the values at  $p_{c1}$ ; open circles are measured at  $p_{c2}$ . The horizontal line indicates the accepted value,  $\gamma/\nu = \frac{43}{24}$ .

the entire range  $0.1 < r < 100$ , it has the value  $1.69 \pm 0.02$ , which, while somewhat less than the expected value<sup>4</sup>  $\gamma/\nu = \frac{43}{24} \approx 1.79$ , is very consistent. Equation (3.7) has an explicit dependence on  $R_0$ , which follows from the renormalization assumption of Sec. II. It can therefore be used to provide another determination of  $\gamma/\nu$ . Figure 8 shows the extrapolation plot for  $\ln S / \ln R_0$  as a function of  $1/\ln R_0$ , for the four largest lattice sizes. The values obtained,  $\gamma/\nu = 1.78 \pm 0.08$ , are in better agreement with the expected value (shown in Fig. 8 by the horizontal line) than the previous data, but are somewhat wider

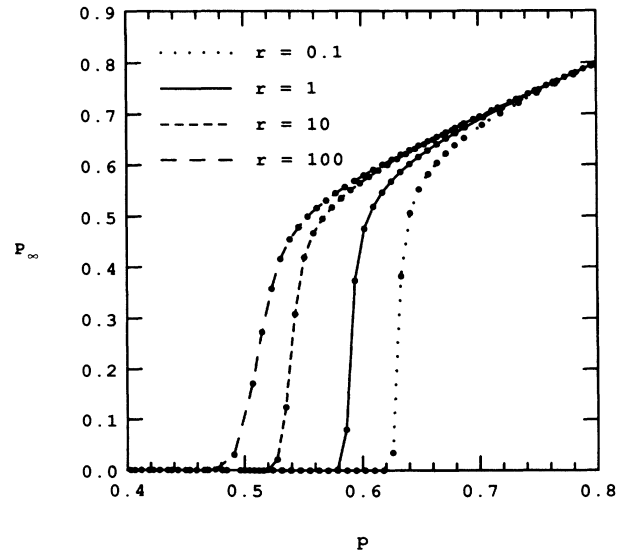


FIG. 9. The infinite cluster density  $P_\infty$  as a function of  $p$ , for several values of  $r$ . The results shown are for a lattice of size  $L = 512$ .

spread. In any case, the near-convergence to a single value and the linear extrapolations visible in Fig. 8 are due to close agreement with the  $R_0$  dependence of (3.7), which implies that the renormalization assumption is, indeed, valid.

The infinite cluster has a density  $P_\infty$  which, near  $p_c$ , is expected to scale like

$$P_\infty \sim |p_c - p|^\beta. \quad (3.8)$$

When  $p_\infty$  is plotted for the different values of  $r$ , as in Fig. 9, the variation of  $p_c$  with  $r$  is again apparent. In a finite system, (3.8) becomes

$$P_\infty(p_c) \sim \left[ \frac{L}{R_0} \right]^{-\beta/\nu}, \quad (3.9)$$

and then the critical exponent ratio  $\beta/\nu$  can be determined as before. From the  $L$  dependence, it is found that  $\beta/\nu = 0.103 \pm 0.005$ , again independent of  $r$ . This is very close to the expected value<sup>4</sup>  $\frac{5}{48} \approx 0.1042$ . From the  $R_0$  dependence,  $\beta/\nu = 0.104 \pm 0.016$ ; the value is again close to the expected result, but the estimated error is much larger. Note that, since  $P_\infty$  is the mass of the infinite cluster  $s_\infty$  per unit volume  $L^d$ , and  $s_\infty \sim L^D$  defines the fractal dimension  $D$ , these results also give an estimate  $D = d - \beta/\nu = 1.897 \pm 0.005$ .

#### IV. CONCLUSIONS

In the preceding sections, an extensive analysis of the cluster-growth model of interactive percolation has been presented. By simple rescaling of the sizes and lengths that exist in the model by the average blob size  $s_0$  and the linear blob size  $R_0$ , respectively, the observed critical behavior in the ferromagnetic and antiferromagnetic regimes can be explained. In every case, the measured exponents are the same as those of random percolation, within the errors. This is strong evidence, therefore, that, despite the presence of interactions in the model, the universality class is unaffected, and at large enough length scales, random percolation is recovered.

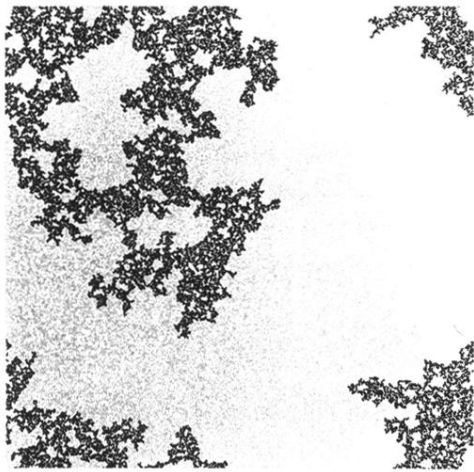
The only case where this may not be true is at the point  $r = \infty$ ,  $p = p_c(\infty)$ , which is similar to the thermal critical point in Ising-correlated percolation in that the correlation length  $\xi$  is divergent in both cases. Unlike the Ising model, however, this point of the phase diagram is unobtainable, since the initial state is  $p = 0$ , and the cluster nucleation probability  $p_0$  is zero.

#### ACKNOWLEDGMENTS

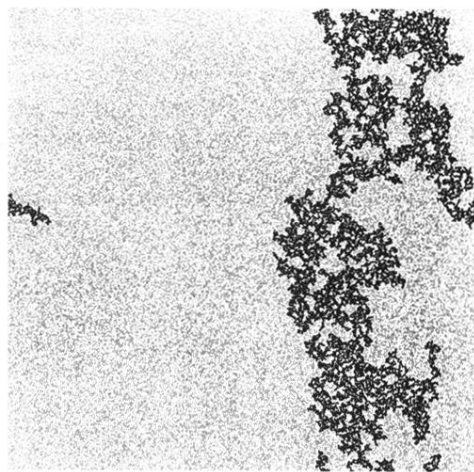
The authors wish to thank Daniel E. Platt, Daniel C. Hong, and M. Daoud for many helpful conversations. This work was supported by the U.S. Office of Naval Research and the Petroleum Research Fund administered by the American Chemical Society.

- <sup>1</sup>D. Stauffer, A. Coniglio, and M. Adam, *Adv. Poly. Sci.* **44**, 103 (1982).  
<sup>2</sup>P. G. de Gennes, *Scaling Concepts in Polymer Physics* (Cornell University Press, Ithaca, 1979).  
<sup>3</sup>M. G. Lagally, G.-C. Wang, and T.-M. Lu, *CRC Crit. Rev. Solid State Mater. Sci.* **7**, 233 (1978).  
<sup>4</sup>D. Stauffer, *Introduction to Percolation Theory* (Taylor and Francis, London, 1985).  
<sup>5</sup>A. Coniglio, C. R. Nappi, F. Peruggi, and L. Russo, *J. Phys. A* **10**, 205 (1977); A. Coniglio and W. Klein, *ibid.* **13**, 2775 (1980).  
<sup>6</sup>Preliminary accounts of this work were presented at the Fall Meeting of the Materials Research Society, Symposium on Fractal Aspects of Disordered Materials, Boston, 1987, and at the March Meeting of the American Physical Society, New Orleans, 1988 [see S. R. Anderson and F. Family, *Bull. Am. Phys. Soc.* **33**, 369 (1988)].  
<sup>7</sup>J. W. Evans, J. A. Bartz, and D. E. Sanders, *Phys. Rev. A* **34**, 1434 (1986).

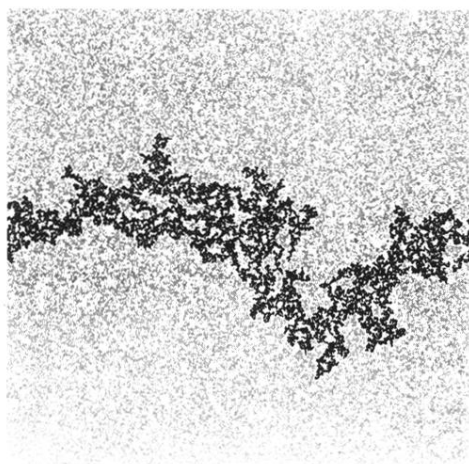
- <sup>8</sup>M. Eden, in *Proceedings of the Fourth Berkeley Symposium on Mathematical Statistics and Probability*, edited by F. Neyman (University of California Press, Berkeley, 1961).  
<sup>9</sup>B. B. Mandelbrot, *The Fractal Geometry of Nature* (Freeman, New York, 1983).  
<sup>10</sup>C. Domb and E. Stoll, *J. Phys. A* **10**, 1141 (1977); A. Coniglio and L. Russo, *ibid.* **12**, 545 (1979).  
<sup>11</sup>E. P. Stoll and C. Domb, *J. Phys. A* **12**, 1843 (1979); A. Coniglio, F. di Liberto, and G. Monroy, *ibid.* **14**, 3017 (1981).  
<sup>12</sup>M. Gouker and F. Family, *Phys. Rev. B* **28**, 1449 (1983).  
<sup>13</sup>J. Kertesz and T. Vicsek, *Z. Phys. B* **45**, 345 (1982).  
<sup>14</sup>*Monte Carlo Methods in Statistical Physics*, edited by K. Binder (Springer-Verlag, Berlin, 1986).  
<sup>15</sup>P. J. Reynolds, H. E. Stanley, and W. Klein, *Phys. Rev. B* **21**, 1223 (1980).  
<sup>16</sup>M. E. Fisher, in *Proceedings of the International School of Physics "Enrico Fermi," Course LI, Varenna, 1970*, edited by M. S. Green (Academic, New York, 1971).



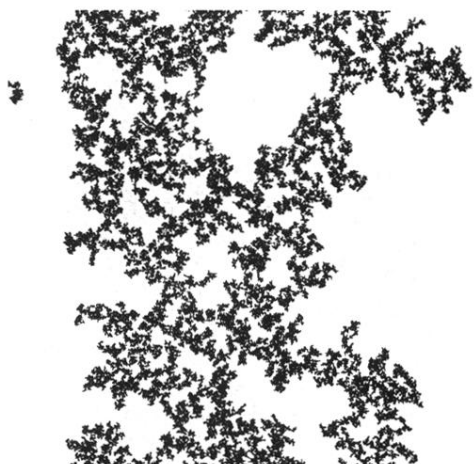
(a)  $r = 0.001$



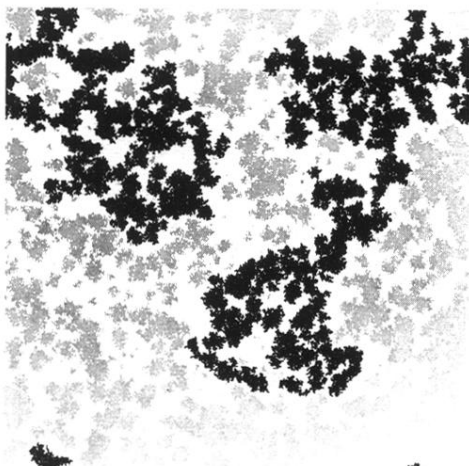
(b)  $r = 1$



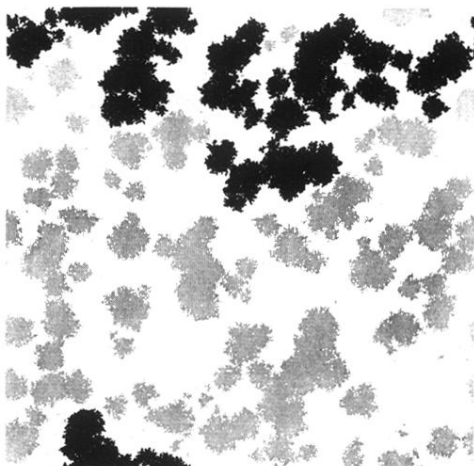
(c)  $r = 10$



(d)  $r = 100$



(e)  $r = 1000$



(f)  $r = 10\,000$

FIG. 2. Sample cluster distributions at the percolation threshold. The infinite cluster is black; all others are gray. (a)  $r = 0.001$ ; (b)  $r = 1$ ; (c)  $r = 10$ ; (d)  $r = 100$ ; (e)  $r = 1000$ ; (f)  $r = 10\,000$ .